ORIGINAL RESEARCH

Optimization of nanoemulsion containing gemcitabine and evaluation of its cytotoxicity towards human fetal lung fibroblast (MRC5) and human lung carcinoma (A549) cells

Nadiatul Atiqah Wahgiman[1]
Norazlinaliza Salim [ID][1,2]
Mohd Basyaruddin Abdul Rahman[1]
Siti Efliza Ashari [ID][1,2]

[1]Integrated Chemical BioPhysics Research, Faculty of Science, University Putra Malaysia (UPM), Serdang, Selangor 43400, Malaysia; [2]Centre of Foundation Studies for Agricultural Science, University Putra Malaysia (UPM), Serdang, Selangor 43400, Malaysia

Background: Gemcitabine (GEM) is a chemotherapeutic agent, which is known to battle cancer but challenging due to its hydrophilic nature. Nanoemulsion is water-in-oil (W/O) nanoemulsion shows potential as a carrier system in delivering gemcitabine to the cancer cell.
Methods: The behaviour of GEM in MCT/surfactants/NaCl systems was studied in the ternary system at different ratios of Tween 80 and Span 80. The system with surfactant ratio 3:7 of Tween 80 and Span 80 was chosen for further study on the preparation of nanoemulsion formulation due to the highest isotropic region. Based on the selected ternary phase diagram, a composition of F1 was chosen and used for optimization by using the D-optimal mixture design. The interaction variables between medium chain triglyceride (MCT), surfactant mixture Tween 80: Span 80 (ratio 3:7), 0.9 % sodium chloride solution and gemcitabine were evaluated towards particle size as a response.
Results: The results showed that NaCl solution and GEM gave more effects on particle size, polydispersity index and zeta potential of 141.57 ± 0.05 nm, 0.168 and -37.10 mV, respectively. The optimized nanoemulsion showed good stability (no phase separation) against centrifugation test and storage at three different temperatures. The in vitro release of gemcitabine at different pH buffer solution was evaluated. The results showed the release of GEM in buffer pH 6.5 (45.19%) was higher than GEM in buffer pH 7.4 (13.62%). The cytotoxicity study showed that the optimized nanoemulsion containing GEM induced cytotoxicity towards A549 cell and at the same time reduced cytotoxicity towards MRC5 when compared to the control (GEM solution).
Keywords: gemcitabine, water-in-oil nanoemulsion, hydrophilic drug, lung cancer, D-optimal mixture design

Introduction

Based on American Cancer Society (2012), lung cancer occurs when a healthy cell in the lung undergoes changes and transforms into the cancer cell and starts to multiply and grows out of control in one or both lungs. This causes the formation of tumour and inefficiency of its function as the lungs provide oxygen to the body via the blood. The total cancer cases reported were 1.6 million cases (13%) from overall global prevalence, and 1.4 million (18%) cancer-related deaths worldwide is lung cancer.[1] The long-term survival rate for the advanced stage of lung cancer is five-year (less than 10%) even with advanced medical science field.[2] Current

Correspondence: Norazlinaliza Salim
Integrated Chemical BioPhysics Research, Faculty of Science, University Putra Malaysia (UPM), Serdang, Selangor 43400, Malaysia
Tel +60 38 946 7807
Email azlinalizas@upm.edu.my

treatments used to treat lung cancer such as surgery, radiation therapy and chemotherapy-targeted therapy are reported. The combination of treatment was also applied to treat cancer depending on the size of a tumour. For example, a combination of chemotherapy and radiation therapies which use a therapeutic agent to inhibit the cancer cell. Many therapeutic agents were used for lung cancer treatment. For example, cisplatin, doxorubicin, quercetin, curcumin and gemcitabine.[3–5]

Gemcitabine (GEM) has been used as chemotherapeutics drug for various solid tumours such as lung cancer, pancreatic cancer, breast cancer, bladder cancer and colon cancer[6,7] which approved by Food and Drug Administration (FDA). GEM has been used in the first line treatment and has excellent therapeutic activity (median overall survival was three months with gemcitabine) in chemotherapy for non-small cell lung cancer (NSCLC).[5,8,9] However, it has very short half-life which is 8–17 min in human plasma and 9 min murine plasma,[9,10] which unfavourable pharmacokinetic and pharmacodynamics profiles as well as poor penetration in the complex environment of lung cancer.[2] Due to the hydrophilic nature of GEM, it is difficult to pass through plasma membrane passively (Wang et al, 2016). Most of the studies on human used higher dosage (1000–1250 mg/m^2, 2 to 3 times for 3 weeks) to achieve therapeutic drug level by intravenous infusion.[5,11–13] To overcome these problems, a delivery system needs to be developed in order to enhance GEM to pass through the plasma membrane.

A pulmonary delivery route is a potential approach towards enhancing the efficiency of treatment with lower toxicity effect towards the normal cell. Pulmonary delivery by inhalation shows good potential for lung cancer as it provides some advantages which do not pass through the first-pass metabolism, fewer side effects of systemic and better compliance to patients as free needle approach.[4,13,14] The particle size of molecules is essential in order to deliver the drug to the targeted cells. The particles between 10 and 20 nm in size deposited to the alveolar region are about four times more efficient than those several microns in diameter.[15] The smaller the particles are, the more efficient the delivery, It could be however depending on the delivery system used. For example, the effect of the size of liposome to deliver the drug via inhalation had been studied by Garbuzenko et al (2014).[16] The results showed that lung concentration of 600 nm and 200 nm liposomes at 3 and 24 h after inhalation was almost 4.5 and 23 times higher when compared with one h (both had practically identical distribution profile).

Nanoemulsion is an emulsion system where they have a particle size less than 200 nm and consist of oil, surfactant and water with an isotropic appearance.[18,19] Nanoemulsion system showed compliance towards the requirement for pulmonary delivery administration. For example, docetaxel-loaded nanoemulsion has been reported with high inhibition (50% reduction of A549 when exposed to 76.41 µg/mL) of the lung cancer cell.[3] From the literature, nanoemulsion does not prolong the half-life of GEM, but it provides shelf-life and long-term stability to arrive at the targeted area and also for storage.[20] As general, nanoemulsion protection the drug from degradation and UV light.[20,21] Other advantages of nanoemulsion include ease of preparation, the stability of thermodynamic and increase of surface area due to fine particle size.[22] Nanoemulsions have the potential to deliver active compounds to the lungs as they provide high drug loading efficiency (1.5 mg/mL of budesonide; 0.05% of quercetin in nanoemulsion).[4,23] Furthermore, they can improve pulmonary deposition and retention leads to prolongment of periods in the lung tissues.[24] Thus, in this study, gemcitabine-loaded nanoemulsion formulation was formulated and optimized for lung cancer treatment. The physicochemical characteristics of the optimized nanoemulsion were investigated. This was followed by the release of in vitro drug and the evaluation of cytotoxicity of the optimized nanoemulsion

Materials and methods
Materials
Gemcitabine (GEM, purity >90%) was purchased from Sigma-Aldrich (Germany). Polysorbate 80 (Tween 80), sorbitan mono-laurate 80 (Span 80) and sodium chloride (NaCl) were purchased from Merck (Germany). Methanol (95%) and acetonitrile (HPLC grade, 99%) were obtained from J.T. Baker Chemical (USA). Medium-chain triglyceride (MCT) was purchased from Gattefosse Sas (France). The human lung fibroblast (MRC5) and human lung cancer carcinoma cell line (A549) was purchased from American Type Culture Collection (ATCC, USA). The deionised water was prepared using Mili-Q filtration system, EMD MiIlipore (Billerica, MA, USA).

Constructions of the ternary phase diagram
NaCl solution was prepared by dissolving 0.9 g of NaCl into 100 mL of deionised water. GEM (0.15 g) was dissolved in 14.85 g of NaCl solution. Tween 80 and Span 80 were mixed at ratio 1:1. The mixed surfactants and medium chain

triglyceride (MCT) were weighed at various ratios ranging from 0:100 to 100:0. Then, the mixture with a total weight of 0.5000 g was placed into a 10 mL screw-cap glass tube (total of 11 tubes) and was vortexed using a vortex mixer (VM-300, Gemmy Industrial CORP-Taiwan). The mixture was centrifuged at 4000 rpm using a Hettich centrifuge (Model EBA, Germany) for 15 min at room temperature. GEM mixture (dissolved in NaCl solution) (1%, w/w) was then added into the eleven test tubes separately and were vortexed for homogenised. The samples were centrifuged at 4000 rpm for 15 min and then observed by the naked eyes for identification of physical phase appearance. The transparent/translucent appearance sample was considered as isotropic, L_t, while milky until separation layers formed was regarded as a multilayer, M. The steps were repeated with the addition of 10, 20, 30, 40 until 90% w/w of gemcitabine solution. These methods were repeated for different surfactant ratios (Tween 80: Span80) of 3:7 and 3:2 with the HLB values were 7.51 and 10.75, respectively. The ternary phase diagrams were constructed using a CHEMIX School v3.6 software (UK).

Preparation of nanoemulsion containing gemcitabine

The combination of high energy and low energy emulsification techniques were used to prepare nanoemulsion. GEM was dissolved in NaCl solution. The mixture was mixed with a mixed surfactant (Tween 80 and Span 80) at room temperature to form an aqueous phase. MCT was sonicated (10 min), heated at 60 °C and stirred using a magnetic bar at 200 rpm for 10 min and homogenised using high shear homogeniser at 6000 rpm for 3 min. MCT was added dropwise into a beaker containing an aqueous phase. The mixture was then homogenised again at 300 rpm for 4 h using overhead stirrer (IKA@ RW 20 Digital, Nara, Japan).

Experimental design

The composition of nanoemulsion formulation was optimized by using D-optimal mixture design. Design-Expert, Version 7.1.5 (Stat-Ease Inc., Minneapolis, USA) was used to analyse the results statically. While the lower and higher limit of the independent variables were determined from the ternary phase diagram. The composition limits of the formulation were listed in Table 1. The independent variables of NaCl solution, GEM, MCT and mixed surfactant (Tween 80: Span 80) were utilised to study the effect of a response variable, particle size. The interactions between independent variables and response were plotted and shown in three-dimensional (3D) surface graphs.

The study of the significant difference between the independent variables was carried out by analysis of variance (ANOVA) and R^2 (coefficient of determination). The criteria of the good reduced model with high correlation, p-value significant ($p<0.0500$) and R^2 value higher than 0.900 were evaluated.

Verification of the model

Several random formulations were prepared and then compared quantitatively on the response variable by calculating their residual standard error (RSE, %) using the equation shown in Equation 1. RSE values lower than 5 % was also in agreement with the predicted values.[25]

$$RSE(\%) = |(\text{Experimental value} - \text{Predicted value})/(\text{Predicted value})| \times 100\% \quad (1)$$

Physicochemical characterisation of the optimized nanoemulsion

Particle size and polydispersity index measurement

The particle size and polydispersity index (PDI) of the nanoemulsion were measured by using Zetasizer Nano ZS (Malvern Instrument Ltd., UK) at 25 °C. The measurement was performed using a dynamic light scattering technique with a scattering angle of 173°. The samples were diluted with MCT (1:500) and injected into the sample cell. The intensity distribution was used for the measurement of the mean average (z-average) particle size. The measurement was repeated in triplicate.

Table 1 The limit of independent variables compositions

Symbol	Variables	Range (% w/w)	
		Lower	High
A	Sodium chloride solution (NaCl solution)	2.80	3.00
B	Gemcitabine (GEM)	0.02	0.04
C	Tween 80: Span 80 (T80:S80, (at ratio 3:7))	15.00	18.00
D	Medium chain triglyceride (MCT)	78.96	82.18

Zeta potential measurement

Zeta potential of the optimized nanoemulsion was measured by using Zetasizer Nano ZS (Malvern Instrument Ltd., UK) at 25 °C. The calculation of their zeta potential was based on their electrophoretic mobility of dispersed particles in a charged field. The stability of nanoemulsion improved as it had zeta potential values higher than +30 mV or lower than – 30 mV.[26] The samples were diluted with MCT (1:500). The measurement was repeated in triplicate.

Transmission electron microscopy analysis

The morphology of the optimized nanoemulsion was visualised using a Transmission Electron Microscope (TEM). The sample was diluted with deionised water and dropped into a 300-mesh formvar-coated copper grid (left at 25 °C for 3 mins) and negatively stained using 2% w/w phosphotungstic acid (left at 25 °C for 5 mins). Meanwhile, the excess liquid was removed with a piece of Whatman filter paper and dried at room temperature. The samples were observed with Hitachi H-700 TEM (Japan) while the acquired digital images were processed with Adobe Photoshop® software.

Drug loading efficiency

The efficiency of GEM loaded in optimized nanoemulsion was determined by the ultrafiltration method. The Centrisart tube (molecular weight cut-off 10,000 Da, Sartorious, AG, Germany) was used to separate the aqueous phase and oil phase. It consists of a floater and centrifugal tube. Optimized nanoemulsion was placed in a floater and centrifuged at 4000 rpm for 15 min. aqueous phase was passed through floater through the filter while the oil phase remained in the floater. Both phases were measured using high performance liquid chromatography (HPLC) measurement (Waters Corporation, Milford, MA) which was equipped with Phenomenex reverse phase C18 column (Gemini, LC column C18, 5µm, 250×4.6 mm) and UV/Vis detector (Waters 2489, Waters Corporation, Milford, MA) at wavelength 269 nm. The Eq 2 below was used to determine the drug loading efficiency:

$$\text{Drug loading efficiency }(\%) = [(W_{initial} - W_{obtained})/W_{initial}] \times 100\% \quad (2)$$

where $W_{initial}$ is the amount of drug present and $W_{obtained}$ in the concentration from oil phase of the optimized nanoemulsion.

Stability study

Centrifugation test was used whereby the fresh sample was centrifuged at 4000 rpm for 15 mins, and any precipitated formed was observed. The storage stability against particle size was evaluated in three different temperatures (4, 25 and 45 °C). The instability mechanisms of the particle size were analysed by coalescence and Ostwald ripening analysis. Coalescence is the process of thinning and disruption of the liquid film between the droplets with the result of the fusion of two or more droplets into larger ones.[17] Coalescence rate can be analysed by plotting the changes in particle size over time. All data obtained from the storage stability of those three different temperatures were applied in the Equation 3.

$$1/r^2 = 1/(r°) - (8\pi/3)\omega t \quad (3)$$

Where r is the average radius of particle size after a certain time, ω is the frequency of rupture per unit of the film surface, while $r°$ is the value at time t=0. A graph of $(1/r^2, nm^{-2})$ against time (seconds) was plotted. Ostwald ripening is the increment of the particle size due to the diffusion of the oil phase through the aqueous phase. Ostwald ripening rate can be determined using Lifshitz–Slesov–Wagner theory, as shown in Eq 4.

$$\omega = dr^3/dt = 8/9[C(\infty)\gamma VmD/\rho RT] \quad (4)$$

Where, ω is the frequency of rupture per unit surface of the film, r is the average radius of the droplets over time, t is the storage time in seconds, C (∞) is the bulk phase solubility, Vm is the molar volume of the internal phase, D is the diffusion coefficient of the dispersed phase in the continuous phase, ρ is the density of the dispersed phase, R is the gas constant, and T is the absolute temperature. Graph of radii (r^3, nm^3) against storage time (t, seconds) at different temperatures were plotted and compared.

In vitro permeation study

The drug release was determined using by Franz diffusion cells method as it mimicked the air-liquid interface present in the lung.[27,28] Cellulose acetate membrane (13 mm, 0.64 cm², 0.45 µm) was clamped between two compartments (donor and receptor compartments) and clipped tightly to prevent leakage. The receptor compartment was filled with 5 mL of phosphate buffer saline (PBS) at pH 7.4. The PBS was sunk at condition temperature of 37±2 °C of temperature along with process studies (48 hrs) and stirred at a speed of 600 rpm for 48 hrs. The optimized nanoemulsion formulation (0.2 mL, C_0=800 µg) was put on the top of the donor compartment. At regular time intervals, 0.5 mL of sample was withdrawn from the receptor compartment and immediately replaced with fresh PBS to maintain the same condition. The samples were kept in the fridge (4 °C) to preserve GEM.

These procedures were repeated by replacing PBS with sodium dihydrogen phosphate buffer (PB) at pH 6.5. These procedures have been studied in order to correlate the effect of pH towards the drug release.

A high-performance liquid chromatography (HPLC) measurement (Waters Corporation, Milford, MA) was equipped with Phenomenex reverse phase C18 column (Gemini, LC column C18, 5 µm, 250×4.6 mm) and UV/Vis detector (Waters 2489, Waters Corporation, Milford, MA). The mobile phase used to analyse GEM release at pH 7.4 was the ratio of phosphate buffer saline and acetonitrile (PBS: ACN, 93:7) at flow rate 1 mL/min at wavelength 269 nm and ambient temperature. The concentration of GEM released was determined based on the standard curve of known GEM with concentration range 20–1000 µg/mL (R^2=0.9907). These methods were repeated by replacing mobile phase PBS with PB (PB: ACN, 93:7) to analyse GEM release at pH 6.5. The concentration of GEM released was determined based on the standard curve of known GEM with concentration range 20–1000 µg/mL (R^2=0.9974). All experiments were carried out in triplicate.

Kinetic measurement

The kinetic measurement of GEM release from optimized nanoemulsion was determined by the mathematical models, zeroth- order (cumulative amount of drug release against time, Eq 5), first-order (log cumulative amount of drug remaining against time, Equation 6), Higuchi (cumulative percentage of drug release against square root of time, Eq 7), Hixson-Crowell (cube root cumulative amount of drug remaining against time, Eq 8) and Korsmeyer-Peppas (log cumulative percentage of drug release against log time, Eq 9).[4] The best model fitted the release data was evaluated based on the coefficient determination (R^2) obtained from plotted graph. The models were constructed based on the model's theoretical equation.

$$M^0 = M^0 + k^0 t \qquad (5)$$

$$\ln M^0 = \ln M^0 + k^1 t \qquad (6)$$

$$M^0 = k_H \sqrt{t} \qquad (7)$$

$$M^{0\frac{1}{3}} - M^{0\frac{1}{3}} = k_w t \qquad (8)$$

$$M^0 / M^0 = k_m t^n \qquad (9)$$

where M^0 is the initial amount of GEM in dissolution media, M_t the amount of GEM released in time, k^0, k^1,

k_H, k_m release rate constants, M^0/M^0 the fraction of GEM release over time, n the release exponent, ant t the time.

Cytotoxicity studies of the optimized nanoemulsion

MTT assay (3- [4, 5- dimethylthiazol-2-yl]-2, 5-diphenylte-trazolium bromide) on human lung fibroblast (MRC5) and human lung cancer carcinoma cell line (A549) was used to determine cytotoxicity. The concentration of 2×10^3 cells/mL of cell culture was prepared and plated onto 96-well plates (100 mL/well). The diluted ranges concentrations (500, 200, 100, 50, 20, 1 µg/mL) of control (GEM solution) were added to each well and it was incubated for 48 and 72 h. MTT solution was added by the end of incubation samples to the cells and continued for incubation in an incubator for 3 h and was replicated in triplicate. After purple formazan crystals solubilised completely in dimethyl sulfoxide (DMSO), the optical density (OD) of the samples was measured using an ELISA reader at a wavelength of 570 nm. The percentage of cell viability was determined using Eq 10.

$$\text{Cell vialability} = ((\text{Absorbance of sample}) /$$
$$(\text{Absorbance of control})) \times 100\% \qquad (10)$$

Graphs were plotted with the percentage of cell viability against their respective concentrations. This method was repeated by replacing the control with nanoemulsion without GEM and optimized nanoemulsion.

Statistical analysis

The statistical analyses of the experiments were performed using analysis of variance (ANOVA) which are Type I *t*-test (least significant different, LSD) and Duncan's Multiple Range Test by using SAS 9.4 software. The value of *p*<0.05 was considered significant. All experiments were carried out triplicate. The error bars represent the mean values with standard deviation (SD) unless otherwise indicated.

Results and discussion
Phase behaviour of mct/surfactants/nacl system

The aqueous phases used to construct ternary phase diagram was sodium chloride solution (0.9 %) with a various ratio of the surfactant of Tween 80 and Span 80 (1:1, 3:2, 3:7) which indicated different HLB values (9.65, 10.75 and 7.51, respectively).

Figure 1A–C, they show isotropic region obtained at maximum 14% of GEM in NaCl solution. Those three of phase diagram gave different amount of percentage area of isotropic (Figure 1A = 13%, Figure 1B= 15%, Figure 1C
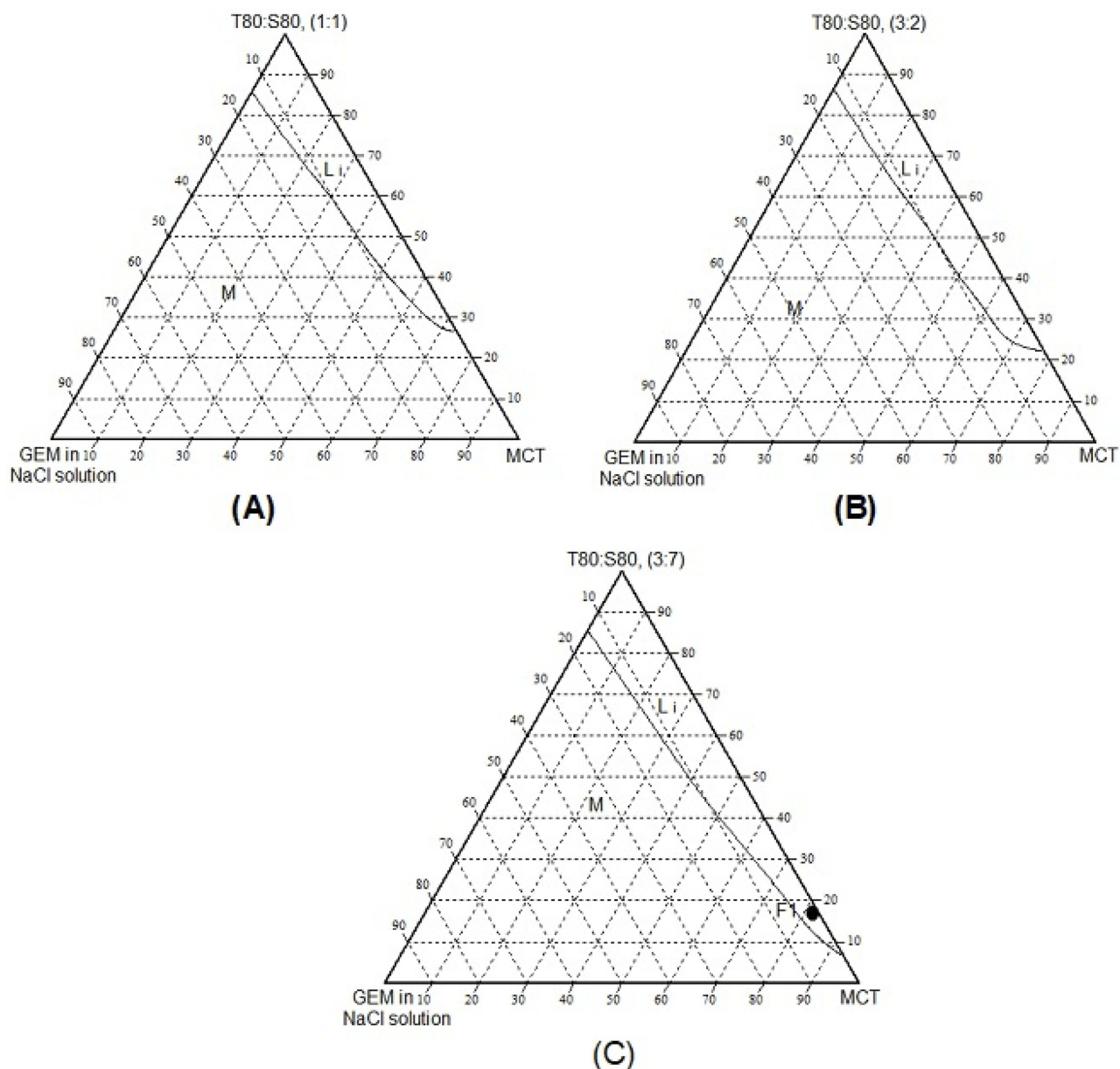
Figure 1 The ternary phase diagrams of MCT/surfactant/NaCl: GEM systems at different Tween 80: Span 80, T80:S80 ratios; (**A**) 1:1 (**B**) 3:2 (**C**) 3:7. Li = Isotropic phase and M = multiple phase.

=16%) and minimum usage of surfactant to form isotropic (Figure 1A = 25%, Figure 1B =20%, Figure 1C = 10%). Figure 1C has 7.51 of HLB value, which is higher lipophilicity and tends to dissolve in oil (MCT). Thus the least amount of mixed surfactant (10%) can form isotropic formulation. While Figure 1A and B have higher HLB value (9.65, 10.75); they are more hydrophilic and dissolve more in water.

The F1 in Figure 1C (T80: S80 ratio at 3.7) was chosen for optimization of the nanoemulsion formulation containing GEM, as it shows the lower percentages

of surfactant in the isotropic region. The higher amount of surfactant used can cause cytotoxicity towards the normal cell. Thus the minimum amount should be used.[29,30] The composition was showed as in Table 2.

Optimization of the nanoemulsion formulation containing GEM

The effects of four independent variables on the actual and predicted particle size of nanoemulsion values were shown in Table 3. The evaluation of the coefficient significance of models was determined by the analysis

Table 2 The composition of the selected point for MCT/surfactants/NaCl system

	Composition (% w/w)
Sodium chloride (NaCl)	0.0398
Water	1.9602
Gemcitabine (GEM)	0.0300
T80: S80	18.0000
Medium-chain triglyceride (MCT)	79.0036

Abbreviations: T80: S80, Tween 80 and Span 80 (at ratio 3:7).

of variance (ANOVA), as shown in Table 4. The F-values and p-value of this model were 47.2694 and <0.0001 respectively. These results showed significant to the particle size. In this model, the R^2, adjusted R^2 and standard deviation of the reduced model are 0.9822, 0.9614 and ±1.89, respectively. The Eq 11 for the model describing the particle size obtained from the model can be written as:

$$Y = -16639.51A + 1279.76B + 128.73C + 120.89D \\ + 86114.41AB + 17907.66AC \\ + 17563.55AD + 1189.64BD$$

D-optimal design analysis

Figure 2(A) shows that as the NaCl solution increased, the particle size increased. This phenomenon happened because of the higher presence of ions from NaCl solution which is known as electrolytes. The presence of electrolytes could lower the attractive forces between water droplets which decrease dielectric constant of the aqueous phase and reduce collision frequency, hence stabilised the droplets[31,32] which also increase of particle size. As for Figure 2(B), the particle size decreased as the surfactant (T80: S80) increased which leads to reduce the interfacial tension and reduction of Laplace pressure and stress.[4,33,34]

Based on Table 5, the composition of the validation set used where the actual particle size and predicted particle size showed agreement as their RSE of five set validations were below 2.72%, which indicated that the model was fitted to the system.

The predicted value of particle size for optimized nanoemulsion was 143.54 nm while the actual value was 141.57±0.05 nm with RSE of 1.37%.

Physiochemical characterisation of the optimized nanoemulsion

The particle size distribution of the optimized nanoemulsion containing GEM obtained was 141.57±0.05 nm,

Table 3 The predicted and actual particle size values of nanoemulsions

	A	B	C	D	Particle size, nm	
					Actual	**Predicted**
1	2.800	0.020	16.500	80.680	124.800	124.800
2	2.900	0.030	16.500	80.570	149.900	149.900
3	2.800	0.040	18.000	79.160	138.800	138.800
4	3.000	0.020	18.000	78.980	130.200	130.200
5	2.800	0.040	18.000	79.160	132.800	132.800
6	2.900	0.040	15.000	82.060	155.800	155.800
7	2.900	0.030	18.000	79.070	157.100	157.100
8	3.000	0.040	18.000	78.960	154.800	154.800
9	2.900	0.020	16.500	80.580	138.00	138.000
10	2.900	0.030	16.500	80.570	149.800	149.800
11	2.950	0.035	17.250	79.765	152.800	152.800
12	3.000	0.020	15.000	81.980	130.000	130.000
13	2.900	0.025	17.250	79.825	146.500	146.500
14	3.000	0.030	16.500	80.470	134.900	134.900
15	2.800	0.030	15.000	82.170	128.500	128.500
16	2.900	0.030	16.500	80.570	149.400	149.400
17	2.850	0.025	15.750	81.375	135.900	135.900
18	2.800	0.020	18.000	79.180	132.600	132.600
19	2.950	0.025	15.750	81.275	134.300	134.300

Abbreviations: A, Gemcitabine; B, NaCl solution; C, Tween 80 and Span 80(at ratio 3:7); D, medium chain triglycerides.

**Table 4** The analysis of variance (ANOVA) for the model

Source	Means square	F-value	p-value
Model	168.8068	47.2694	<0.0001
Linear mixture	72.0740	20.1822	0.0015
Residual	3.5711	-	-
Lack of fit	1.0956	0.1812	0.9028
Pure error	6.046667	-	-

which valid with predicted value (143.54 nm) as its RSE is 1.37%. The polydispersity index (PDI) of 0.168 was obtained, which indicated a monodisperse system and zeta potential value of −37.10 mV. Figure 3 showed that the optimized nanoemulsion was spherical. The particles were distributed uniformly without aggregation among them, and the particle size obtained agreed with particle size analysis. While the drug loaded in optimized nanoemulsion is 100%.

Stability study

The stability study by centrifugation test and storage stability, have shown that optimized nanoemulsion was stable. A fresh sample of optimized nanoemulsion remained as a homogeneous mixture after centrifuged at 4000 rpm for 15 min, which indicated that it was stable under normal storage condition. For storage stability of three different temperatures, optimized nanoemulsion remained at homogeneous phase after 90 days, as shown in Table 6.

There were increments in particle size after storage for (90 days) which were 51.31% (4 °C), 53.32% (25 °C) and 63.79% (45 °C) as in Figure 4. The plotted graphs (Figs. 5 and 6) show no linear relationship, indicating the increment of particle size over time happened not because of coalescence rate and Ostwald ripening phenomena. Coalescence rate analysis included the linear relationship between $1/r^2$ against storage time in which two droplets fusion formed
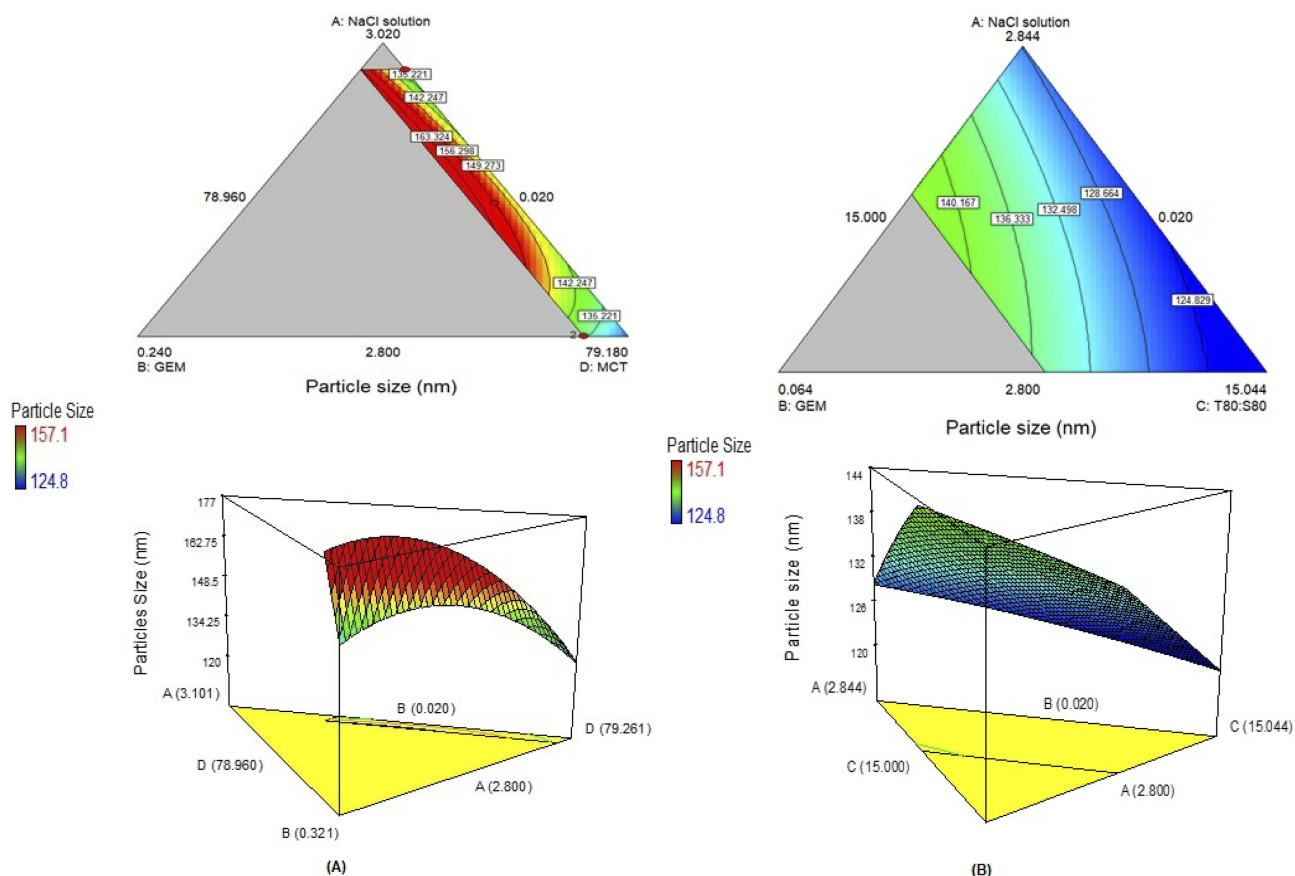

Figure 2 (**A**) The contour plot of two-dimensional plot and three-dimensional surfaces with a constant amount of surfactant (T80: S80 (C)), showing the interaction effect between three variables (NaCl solution (**A**), GEM (B), MCT (D)). (**B**) The contour plot of two-dimensional plot and three-dimensional surfaces with a constant amount of oil (MCT (D)), showing the interaction effect of three variables (NaCl solution (A), GEM (B), T80: S80 (C)).

Table 5 Validation set and optimized nanoemulsion

	A	B	C	D	Particle size		PDI	Zeta potential mV	Residual standard error (%)
					Actual	Predicted			
Validation									
V1	3.00	0.04	16.46	80.50	155.60±0.04	153.44	0.101	–	1.41
V2	3.00	0.04	15.46	81.50	148.40±0.03	146.66	0.176	–	1.19
V3	3.00	0.04	15.96	81.00	153.90±0.30	158.21	0.254	–	2.72
V4	2.90	0.03	17.00	80.07	150.00±0.10	151.89	0.169	–	1.24
V5	2.90	0.03	17.50	79.57	152.30±0.18	154.19	0.042	–	1.23
Optimization									
	3.00	0.04	15.00	81.96	141.57±0.05	143.54	0.168	−37.10	1.37

Abbreviations: A, Gemcitabine; B, NaCl solution; C, Tween 80 and Span 80 (at ratio 3:7); D, medium chain triglycerides.
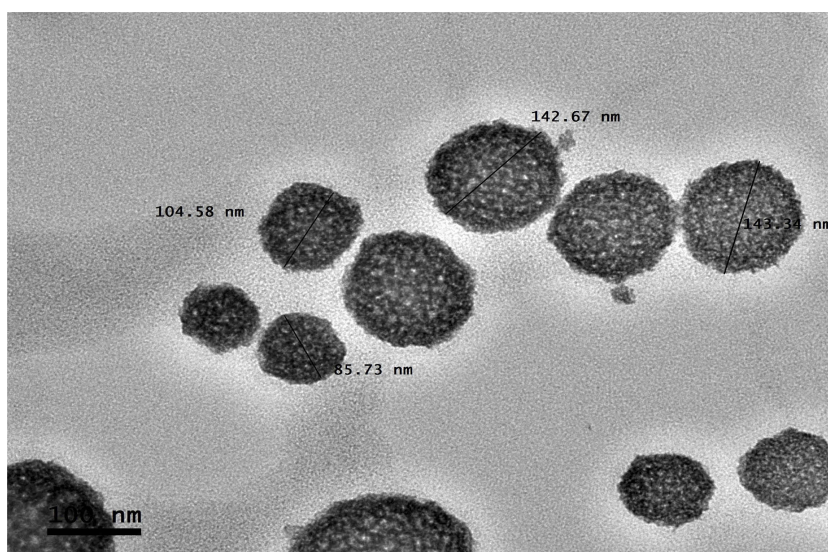
Figure 3 Morphology of the optimized nanoemulsion at 100 nm of magnification.

Table 6 Physical stability of optimized nanoemulsion containing GEM

Temperature (°C)	Stability storage (days)						Centrifugation test
	1	7	21	30	60	90	√
4	√	√	√	√	√	√	
25	√	√	√	√	√	√	
45	√	√	√	√	√	√	

Note: √ No separation.

larger particles as rupture of continuous phase films happened.[38,39] Ostwald ripening was a process expansion of particles in the nanoemulsion system due to curvature effects by absorbing energy from the surrounding.[17,35,36] Particles in the nanoemulsion system gained energy from the surrounding temperature. The higher energy increased the kinetic energy of particles and the efficient collision among particles (Brownian law). Thus, the diffusion that happened led to the increment of particle size.

In vitro permeation study

The in vitro permeation study of optimized nanoemulsion at different pH (pH 7.4 and 6.5) have been studied. Figure 7 showed that the release of GEM at pH 7.4 (13.62%) was
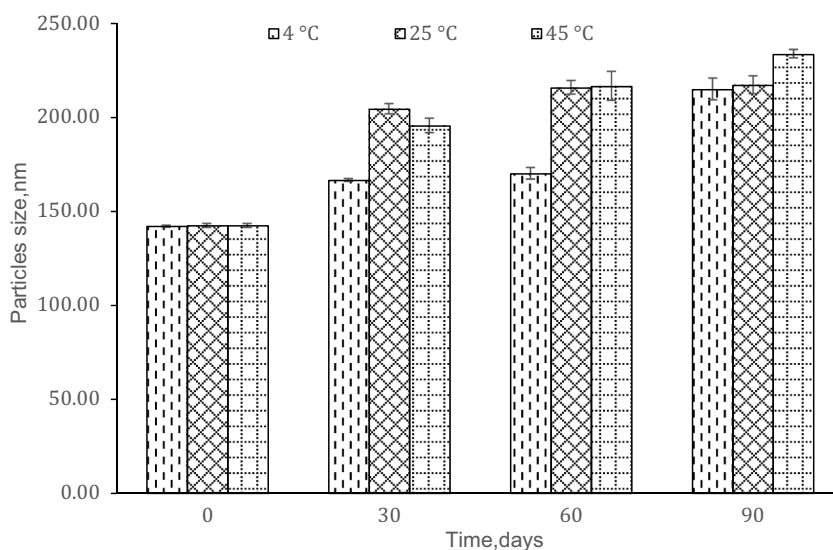
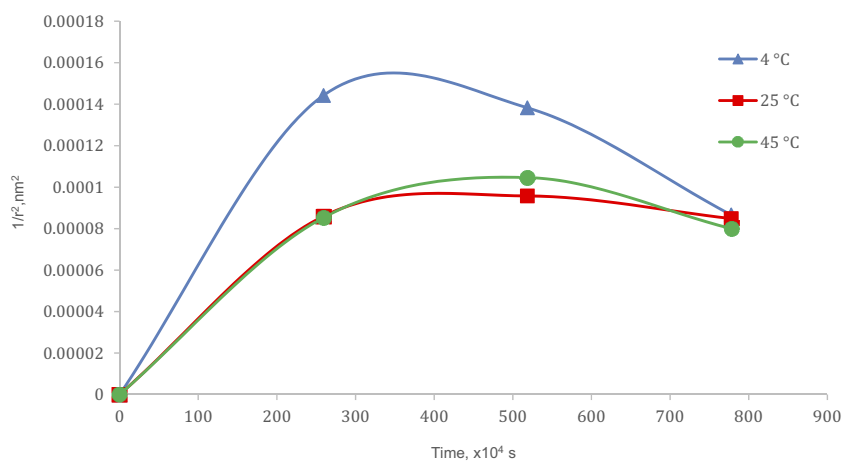**Figure 4** Stability of the optimized nanoemulsion against time.

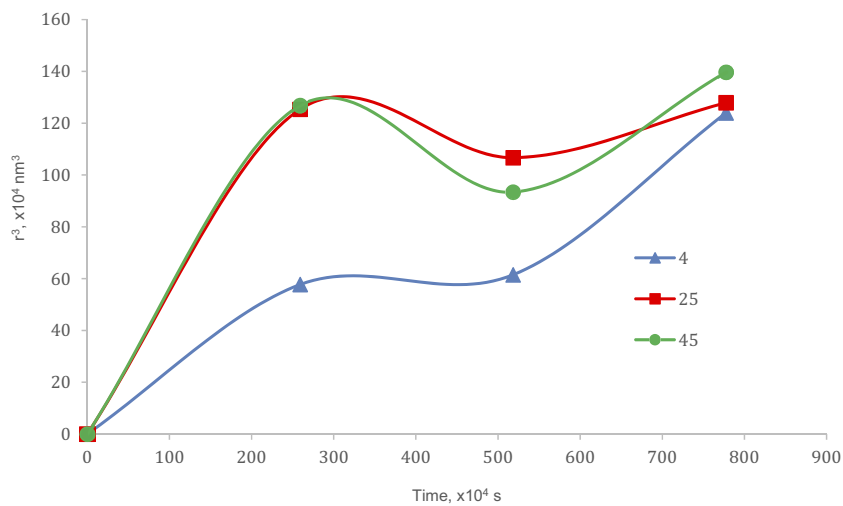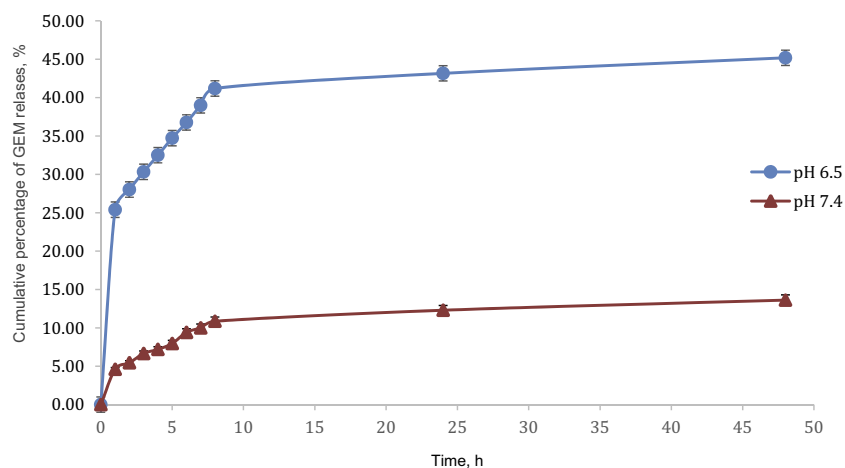**Figure 5** Coalescence rate analysis.

Figure 6 Ostwald ripening analysis.

Figure 7 Graph cumulative percentage release GEM, %.

lower (3-fold) compared to the drug released at pH 6.5 (45.19%) for 48 hrs. In other words, the release of GEM increased significantly with reductions in pH, which similar results were reported by Lee et al (2014).[42] These results indicated the optimized nanoemulsion had a sustained property of release at pH 7.4 (pH value normal lung cell) and an unstained property release at pH 6.5 (pH value lung cancer cell). In addition, the presence of non-ionic polyoxyethylene sorbitan esters (Tween 80 and Span 80), which were to stabilise the emulsion by lowering the surface tension between particles and preventing the coalescence phenomena cause GEM to be retained in nanoemulsion.[37]

Kinetic release analysis

The coefficient of determination (R^2) of all kinetic models for GEM release from optimized nanoemulsion in pH 7.4 and pH 6.5 were shown in Table 7. All plotted graph shows linear relationships to a different degree of time for pH 7.4 and pH 6.5 (Figure 8 and Figure 9). The highest R^2 for pH 7.4 was zeroth order (0.9932) followed by first- order

Table 7 The coefficient of determination (R^2) of all kinetic models for GEM release from optimized nanoemulsion in pH 7.4 and pH 6.5

| Kinetic model	pH 7.4	pH 6.5
	Coefficient of determination (R^2)	
Zeroth- order	0.9932	0.9957
First- order	0.9930	0.9870
Hixson-Crowell	0.9931	0.9909
Higuchi	0.9756	0.9874
Korsmeyer- peppas	0.9673	0.9632

(0.9930), Hixson-Crowell (0.9931), Higuchi (0.9756) and Korsmeyers-Peppas (0.9673). While the highest R^2 for pH 6.5 was zeroth-order (0.9957) followed by Hixson-Crowell (0.9909), Higuchi (0.9874), first-order (0.9870) and Korsmeyers-Peppas (0.9632). The R^2 for GEM release from optimized nanoemulsion in pH 7.4 and pH 6.5 were fitted the most with zeroth-order.

Cytotoxicity study

The cytotoxicity of GEM, nanoemulsion without GEM and optimized nanoemulsion were investigated by MTT assay for 72 hrs on MRC5 and A549 cells. The selection of the cell lines was actually based on the previous study[4,38] Figure 10A and B show the percentage of cell viability of GEM, nanoemulsion without GEM and optimized nanoemulsion when exposed to MRC5 and A549 at concentration 100 to 500 μg/mL. The IC_{50} of GEM, nanoemulsion without GEM and optimized nanoemulsion were listed in Table 8.

GEM exposure at concentration 50 μg/mL and 100 μg/mL induces a statistically significant ($p<0.010$) decreased (49.607% and 50.392%) of the cell viability. The percentage of cell viability decrease as the concentration of GEM increase (1–500 μg/mL). While a statistically significant ($p<0.050$) of reduction of the percentage of cell viability as the increased concentration (100–500 μg/mL). The IC_{50} of GEM exposure on MRC5 and A549 are 70 μg/mL and highly toxic up to the identified concentrations (1 μg/mL).

The nanoemulsion without GEM shows a statistically significant ($p<0.050$) decrease more than 50% percentage cell viability when exposed on MRC5 at concentration 200 μg/mL and 500 μg/mL. The exposure of it on A549 does not induce of the cell viability up to 500 μg/mL. The
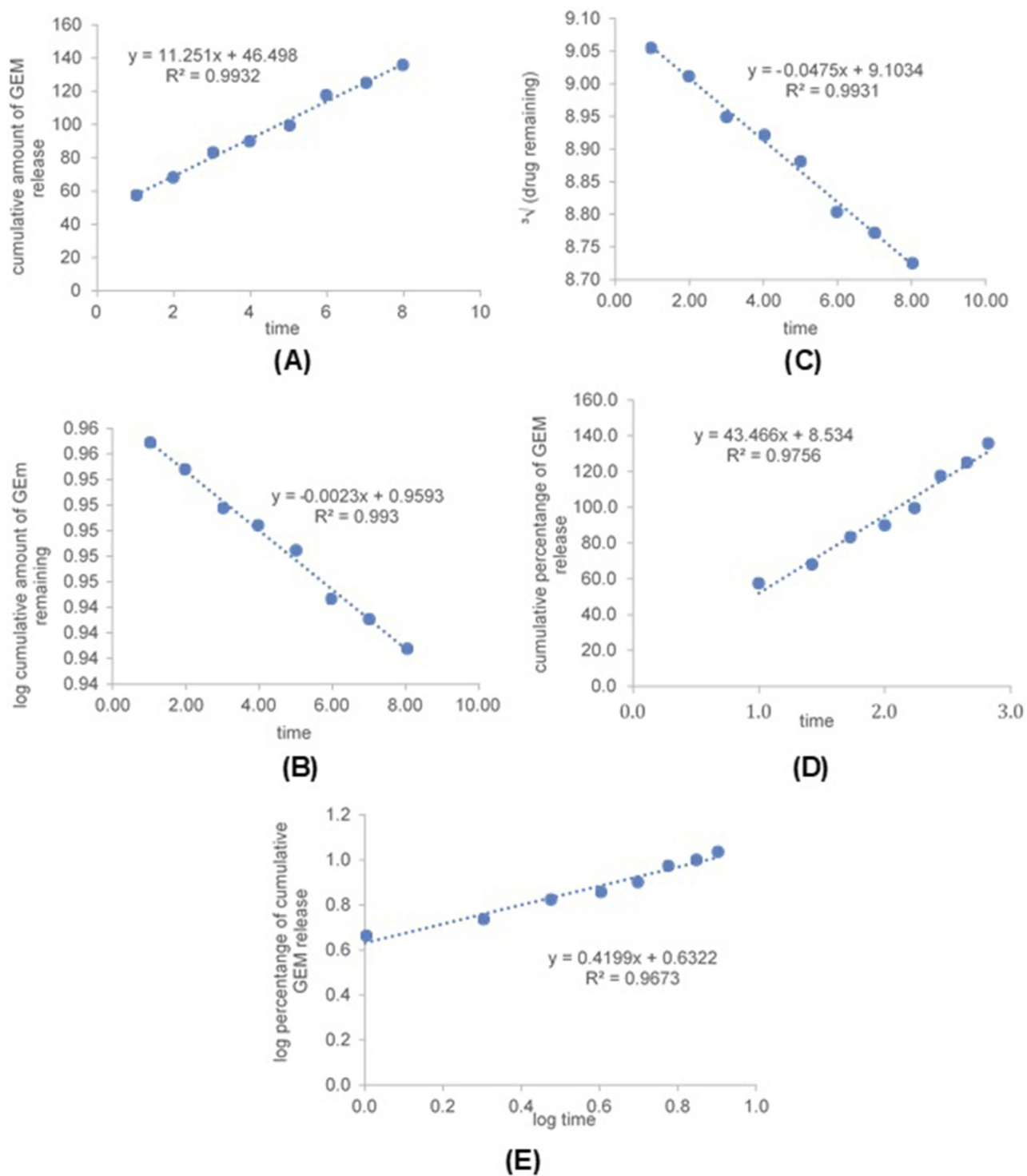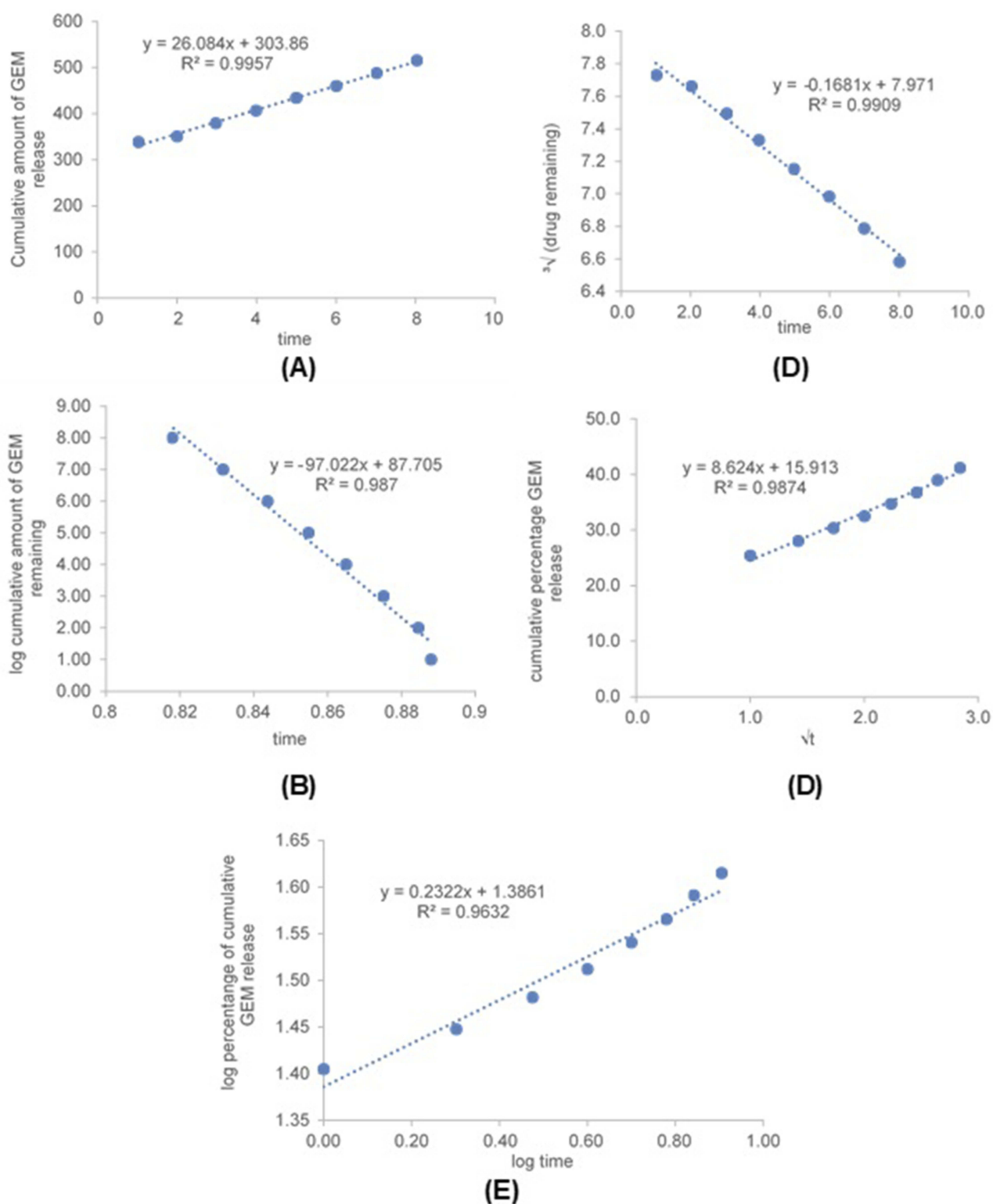
Figure 8 Graph of kinetic models, zeroth-order (**A**) first-order (**B**), Hixson-Crowell (**C**), Higuchi (**D**) and Korsmeyers-Peppas (**E**) for GEM release from optimized nanoemulsion in pH 7.4.

IC_{50} for nanoemulsion without GEM was at 110 μg/mL for MRC5 and not toxic to A549 cell up to 500 μg/mL.

When optimized nanoemulsion exposure to MRC5 at concentration 100 μg/mL and 200 μg/mL induce a statistically significant ($p<0.050$) reduction (48.282% and 55.588%) of cell viability. The optimized nanoemulsion induced cytotoxic response with IC_{50} at 165 μg/mL (MRC5) and 55 μg/mL (A549). Besides,

Figure 9 Graph of kinetic models, zeroth-order (**A**) first-order (**B**), Hixson-Crowell (**C**), Higuchi (**D**) and Korsmeyers-Peppas (**E**) for GEM release from optimized nanoemulsion in pH 6.5.

the optimized nanoemulsion shows the reduction of percentage cell viability due to the increase of sample concentration (Figure 10B). These results of the studies demonstrated that optimized nanoemulsion had the capability to induce cytotoxicity on A549 lung cancer cells.
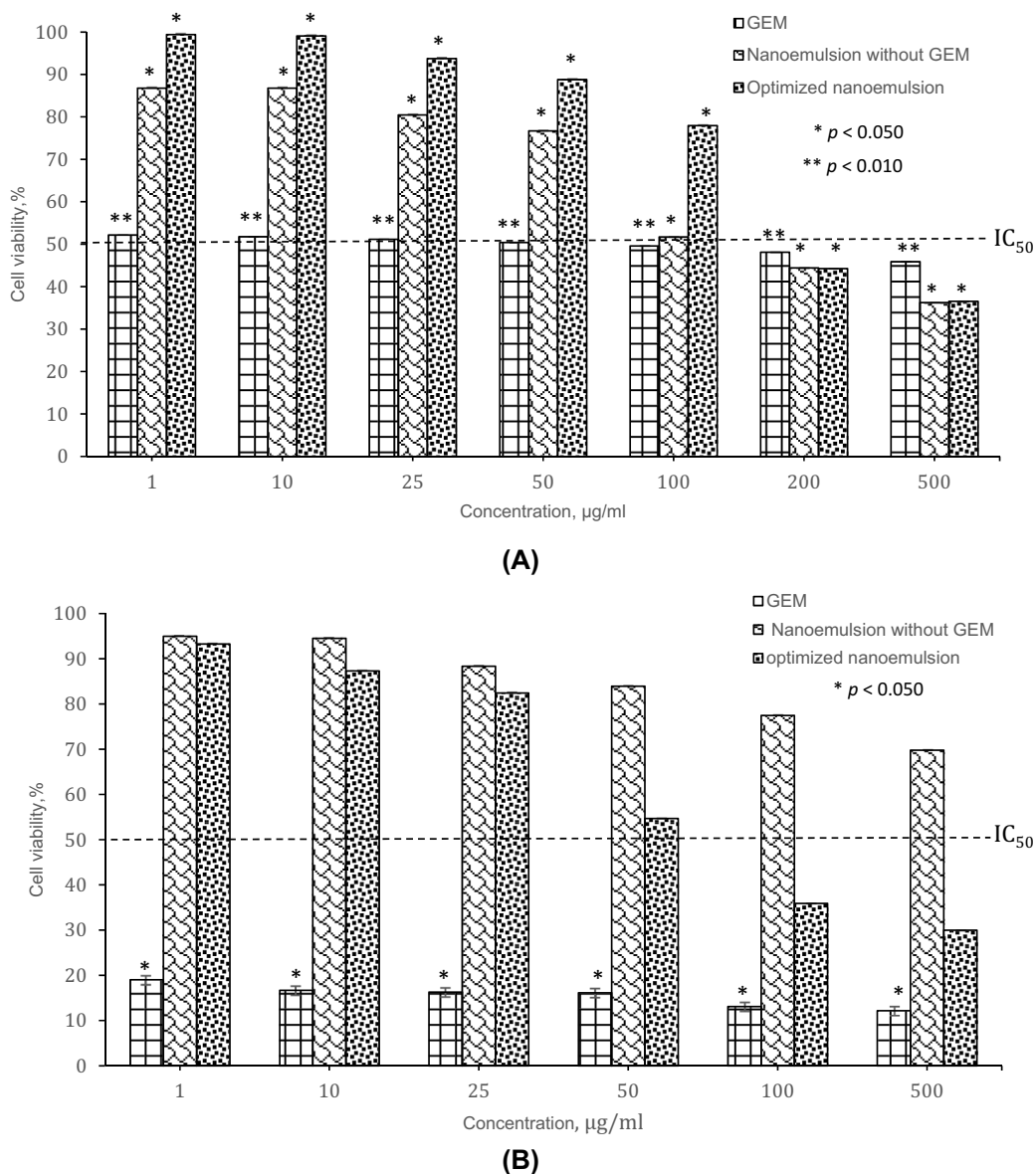
(A)

(B)

Figure 10 The cytotoxicity effect of different cell lines: (**A**) MRC5 lung cells, (**B**) A549 lung cancer cells at 72 h treatment.

Table 8 IC_{50} values for cytotoxicity study

	IC_{50} µg/mL	
	MRC5	**A549**
GEM	70	Highly toxic up to 1
Nanoemulsion without GEM	110	Not toxic up to 500
Optimized nanoemulsion	165	55

Based on Figure 10, there show optimized nanoemulsion shows of reduction of cell viability when it introduced to MRC5 cell and A549 cell because of the presence of GEM. GEM was activated their cytotoxicity activity through the series of phosphorylation intercellularly by deoxycytidine kinase to the monophosphate and the by pyrimidine nucleoside monophosphate kinase to give gemcitabine diphosphate which derives gemcitabine triphosphate by nucleoside diphosphate kinase.[8,39,40] The gemcitabine diphosphate inhibits ribonucleotide reductase, an enzyme that produces the deoxyribonucleotides for DNA synthesis in S phase of dividing cells while gemcitabine triphosphate intermediate into DNA which terminated DNA synthesis.[41] Thus, MRC5 and A549 cells reduced up to 50% at certain concentration when they were introduced to optimized nanoemulsion.

Conclusion

Nanoemulsions containing gemcitabine have been developed by a combination of high and low energy emulsification technique. Based on ternary phase diagrams constructed, the selected formulation was successfully optimized by D-optimal design. The optimized nanoemulsion was obtained with good physical stability against centrifugation test and storage temperatures. The in vitro permeation study obtained 3-fold released towards pH value of lung cancer compare pH value of normal lung cell. Cytotoxicity studies of the optimized nanoemulsion showed that it was toxic to A549 lung cancer cell but less cytotoxicity when compared to GEM only toward lung cancer cell, A549. While on MRC5 normal lung cell, optimized nanoemulsion also less toxic compared to GEM only. These results of studies show optimized nanoemulsion by nanoemulsion system has the potential to enhance the treatment for lung cancer.

Acknowledgment

Disclosure

The authors report no conflicts of interest in this work.

References

1. Dela Cruz CS, Tanoue LT, Matthay RA. Lung Cancer: Epidemiology, Etiology, and Prevention. *Clin Chest Med*. 2011;32(4):605–644. doi:10.1016/j.ccm.2011.09.001
2. Soni N, Soni N, Pandey H, Maheshwari R, Kesharwani P. Augmented delivery of gemcitabine in lung cancer cells exploring mannose anchored solid lipid nanoparticles. *J Colloid Interface Sci*. 2016;481:107–116. doi:10.1016/j.jcis.2016.07.020
3. Asmawi AA, Salim N, Ngan CL, et al. Excipient selection and aerodynamic characterisation of nebulised lipid-based nanoemulsion loaded with docetaxel for lung cancer treatment. *Drug Deliv Transl Res*. 2018;9(2):543–554. doi:10.1007/s13346-018-0526-4
4. Arbain NH, Salim N, Masoumi HRF, Wong TW, Basri M, Abdul Rahman MB. In vitro evaluation of the inhalable quercetin loaded nanoemulsion for pulmonary delivery. *Drug Deliv Transl Res*. 2018;67:497–507.
5. Morabito A, Gebbia V, Di M, et al. Randomized phase III trial of gemcitabine and cisplatin vs. gemcitabine alone in patients with advanced non-small cell lung cancer and a performance status of 2: the CAPPA-2 study. *Lung Cancer*. 2013;81:77–83. doi:10.1016/j.lungcan.2013.04.008
6. Hessmann E, Patzak MS, Klein L, et al. Fibroblast drug scavenging increases intratumoral gemcitabine accumulation in murine pancreas cancer. *Gut*. 2016;67(3):497–507. doi:10.1136/gutjnl-2016-311954
7. Liang T, Zhou Z, Cao Y, Ma M, Wang X, Jing K. Gemcitabine-based polymer-drug conjugate for enhanced anticancer effect in colon cancer. *Int J Pharm*. 2016;513(1–2):564–571. doi:10.1016/j.ijpharm.2016.09.018
8. Bornmann C, Graeser R, Esser N, et al. A new liposomal formulation of Gemcitabine is active in an orthotopic mouse model of pancreatic cancer accessible to bioluminescence imaging. *Cancer Chemother Pharmacol*. 2008;61(3):395–405. doi:10.1007/s00280-007-0482-z
9. Alvarellos ML, Lamba J, Sangkuhl K, et al. PharmGKB summary. *Pharmacogenet Genomics*. 2014;24(11):564–574. doi:10.1097/FPC.0000000000000086
10. Abu-Fayyad A, Nazzal S. Gemcitabine-vitamin E conjugates: synthesis, characterisation, entrapment into nanoemulsions, and *in-vitro* deamination and antitumor activity. *Int J Pharm*. 2017;528:463–470. doi:10.1016/j.ijpharm.2017.06.031
11. Anderson BH, Lund B, Bach F, Thatcher N, Walling J, Hansen HH. Single-agent activity of weekly gemcitabine in advanced non-small-cell lung cancer: a Phase II Study. *Am Soc Clin Oncol*. 1994;12(9):821–1826. doi:10.1200/JCO.1994.12.9.1821
12. Ruiz Van Haperen VWT, Veerman G, Vermorken JB, Pinedo HM, Peters GJ. Regulation of phosphorylation of Deoxycytidine and 2′,2′-difluorodeoxycytidine (Gemcitabine); effects of Cytidine 5′-Triphosphate and Uridine 5′-Triphosphate in relation to Chemosensitivity for 2′,2′-Difluorodeoxycytidine. *Biochem Pharmacol*. 1996;51:911–918. doi:10.1016/0006-2952(95)02402-6
13. Akhter S, Ahmad J, Rizwanullah M, Rahman M, Zaki Ahmad M, Rizvi MMA. Nanotechnology-based inhalation treatments for lung cancer: state of the art. *Nanotechnol Sci Appl*. 2015;8:55–56. doi:10.2147/NSA.S49052
14. Sung JC, Pulliam BL, Edwards DA. Nanoparticles for drug delivery to the lungs. *Trends Biotechnol*. 2007;25:563–570. doi:10.1016/j.tibtech.2007.09.005
15. Onischuk AA, Tolstikova TG, Baklanov AM, Khvostov MV. Generation, inhalation delivery and anti-hypertensive effect of nisoldipine nano aerosol. *J Aerosol Sci*. 2014;78:41–54. doi:10.1016/j.jaerosci.2014.08.004
16. Garbuzenko OB, Mainelis G, Taratula O, Minko T. Inhalation treatment of lung cancer: the influence of composition, size and shape of nanocarriers on their lung accumulation and retention. *Cancer Biol Med*. 2014;11(1):44.
17. Tadros TF. *Emulsion Formation, Stability, and Rheology* (T. F. Tadros, Ed.) 1st ed. Wiley-VCH Verlag Gmbh & Co. KGaA;2013.
18. Jaiswal M, Dudhe R, Sharma PK. Nanoemulsion: an advanced mode of drug delivery system. *3 Biotech*. 2015;5(2):123–127. doi:10.1007/s13205-014-0214-0
19. Salim N, Ahmad N, Musa SH, Hashim R, Tadros TF, Basri M. Nanoemulsion as a topical delivery system of antipsoriatic drugs. *RSC Adv*. 2016;6:6234–6250.
20. Khan I, Bahuguna A, Kumar P, Bajpai VK, Kang SC. In vitro and in vivo antitumor potential of carvacrol nanoemulsion against human lung adenocarcinoma A549 cells via mitochondrial-mediated apoptosis. *Sci Rep*. 2018;8(1):712–714.
21. Choudhury H, Gorain B, Karmakar S, et al. Improvement of cellular uptake, in vitro antitumor activity and sustained release profile with increased bioavailability from a nanoemulsion platform. *Int J Pharm*. 2014;460(1–2):131–143. doi:10.1016/j.ijpharm.2013.10.055
22. Solans C, Izquierdo P, Nolla J, Azemar N, Garcia-celma MJ. Nanoemulsions. *Curr Opin Colloid Interface Sci*. 2005;10(3–4):102–110. doi:10.1016/j.cocis.2005.06.004
23. Amani A, York P, Chrystyn H, Clark BJ. Evaluation of a nanoemulsion-based formulation for respiratory delivery of budesonide by nebulizers. *Am Pharm Sci Pharm Sci Tech*. 2010;11(3):1147–1151.
24. Nasr M, Nawaz S, Elhissi A. Amphotericin B lipid nanoemulsion aerosols for targeting peripheral respiratory airways via nebulization. *Int J Pharm*. 2012;436:611–616. doi:10.1016/j.ijpharm.2012.07.028

25. Sulaiman CIS, Basri M, Masoumi HRF, Chee WJ, Ashari SE, Ismail M. Effects of temperature, time, and solvent ratio on the extraction of phenolic compounds and the anti-radical activity of Clinacanthus nutans Lindau leaves by response surface methodology. *Chem Cent J.* 2017;11:1–11. doi:10.1186/s13065-017-0351-8

26. Ribeiro RC, Barreto SM, Ostrosky EA, Da Rocho-Filho PA, Verissimo LM, Ferrari M. Production and characterisation of cosmetic nanoemulsions containing Opuntia ficusindica (L.) mill extract as moisturizing agent. *Molecules.* 2015;20(2):2492–2509.

27. Kim SY, Naskar D, Kundu SC, et al. Formulation of biologically-inspired silk-based drug carriers for pulmonary delivery targeted for lung cancer. *Sci Rep.* 2015;5(1):11878. doi:10.1038/srep11878

28. Wyszogrodzka G, Dorożyński P, Gil B, et al. Iron-based metal-organic frameworks as a theranostic carrier for local tuberculosis therapy. *Pharm Res.* 2018;35(7):144. doi:10.1007/s11095-018-2425-2

29. Hwang TL, Fang CL, Chen CH, Fang JY. Permeation enhancer containing water-in-oil nanoemulsions as carriers for intravesical cisplatin delivery. *Pharm Res.* 2009;26(10):2314–2323. doi:10.1007/s11095-008-9767-0

30. Prajapati HN, Dalrymple DM, Serajuddin ATM, et al. Formulation and physiochemical study of a-tocopherol based oil in water nanoemulsion stabilised with non-toxic, biodegradable surfactant: sodium stearoyl lactate. *Ultrason Sonochem.* 2016;29(1):285–305. doi:10.1016/j.ultsonch.2015.09.007

31. Frasch-Melnik S, Spyropoulos F, Norton IT. W1/O/W2double emulsions stabilised by fat crystals: formulation, stability and salt release. *J Colloid Interface Sci.* 2010;350(1):178–185. doi:10.1016/j.jcis.2010.06.039

32. Matos M, Gutierres G, Coca J, Pazos C. Preparation of water-in-oil-water (W/O/W) double emulsions containing trans-resveratrol. *Colloids Surf A.* 2014;442:69–79. doi:10.1016/j.colsurfa.2013.05.065

33. Sood S, Jain K, Gowthamarajan K. Optimization of curcumin nanoemulsion for intranasal delivery using the design of experiment and its toxicity assessment. *Colloids Surf B.* 2014;113:330–337. doi:10.1016/j.colsurfb.2013.09.018

34. Azhar SSNA, Ashari SE, Salim N. Development of a kojic mono-oleate-enriched oil-in-water nanoemulsion as a potential carrier for hyperpigmentation treatment. *Int J Nanomedicine.* 2018;13:6465–6479. doi:10.2147/IJN.S177627

35. Musa SH, Basri M, Masoumi HRF, Karjiban RA, Malek EA, Basri H. Formulation optimisation of palm kernel oil esters nanoemulsion-loaded with chloramphenicol suitable for meningitis treatment. *Colloids Surf B.* 2013;112:1139. doi:10.1016/j.colsurfb.2013.07.043

36. Musa SH, Basri M, Masoumi HRF, Shamsudin N, Salim N. Enhancement of physicochemical properties of nanocolloidal carrier loaded with cyclosporine for tropical treatment of psoriasis: in vitro diffusion and in vivo hydrating action. *Int J Nanomed.* 2017;12:2427–2441. doi:10.2147/IJN.S125302

37. Artiga-artigas M, Lanjari-pérez Y, Martín-belloso O. Curcumin-loaded nanoemulsions stability as affected by the nature and concentration of surfactant. *Food Chem.* 2018;266:466–474. doi:10.1016/j.foodchem.2018.06.043

38. Chang HB, Chen BH. Inhibition of lung cancer cells A549 and H460 by curcuminoid extracts and nanoemulsions prepared from Curcuma longa Linnaeus. *Int J Nanomedicine.* 2015;10:5059–5080.

39. Mini E, Nobili S, Caciagli B, Landini I, Mazzei T. Cellular pharmacology of gemcitabine. *Ann Oncol.* 2006;17:7–12. doi:10.1093/annonc/mdj941

40. Jia Y, Xie J. Promising molecular mechanisms responsible for gemcitabine resistance in cancer. *Genes Dis.* 2015;2(4):299–306. doi:10.1016/j.gendis.2015.07.003

41. Toschi L, Cappuzzo F. Gemcitabine for the treatment of advanced nonsmall cell lung cancer. *Onco Targets Ther.* 2009;2:209–217.

42. Lee W.H, Loo C.Y, Young P.M, Traini D, Mason R.S, Rohanizadeh R. Recent advances in curcumin nanoformulation for cancer therapy. *Expert Opinion Drug Delivery.* 2014;11:1183–1201.